

Preclinical pharmacokinetics and in vitro metabolism of brivanib (BMS-540215), a potent VEGFR2 inhibitor and its alanine ester prodrug brivanib alaninate

Punit H. Marathe · Amrita V. Kamath ·
Yueping Zhang · Celia D'Arienzo · Rajeev Bhide ·
Joseph Fargnoli

Received: 2 October 2008 / Accepted: 7 April 2009 / Published online: 26 April 2009
© Springer-Verlag 2009

Abstract

Purpose Brivanib alaninate is a prodrug of brivanib (BMS-540215), a potent oral VEGFR-2 inhibitor and is currently in development for the treatment of hepatocellular and colon carcinomas. In vitro and in vivo studies were conducted to characterize the preclinical pharmacokinetics and disposition of brivanib and brivanib alaninate, and antitumor efficacy in mice bearing human xenografts. **Methods** In vitro studies were conducted in liver and intestinal fractions, plasma and Caco-2 cells to assess the metabolic stability. Pharmacokinetics of brivanib were determined in preclinical species after administration of single intravenous or oral doses of both brivanib and brivanib alaninate. The antitumor efficacy was assessed at equimolar doses in nude mice bearing human tumor xenografts. Human efficacious dose was predicted based on projected human pharmacokinetic parameters and exposure at efficacious doses in the mouse efficacy models.

Results In vitro and in vivo studies indicated that brivanib alaninate was efficiently converted to brivanib. Brivanib showed good brain penetration in rats consistent with its high intrinsic permeability and lack of active efflux in Caco-2 cells. The oral bioavailability of brivanib varied

among species (22–88%) and showed dissolution rate-limited absorption even when combined with organic co-solvents. Administration of brivanib as brivanib alaninate allowed completely aqueous vehicles, and an improvement in the oral bioavailability (55–97%) was observed. The clearance of brivanib in humans is anticipated to be low to intermediate (hepatic extraction ratio < 0.7), while its volume of distribution is expected to be high. The minimum efficacious dose of brivanib alaninate was determined to be 60 mg/kg per day.

Conclusions Brivanib alaninate is rapidly and efficiently converted to the parent, brivanib, as demonstrated both in vitro and in vivo and offers an excellent mode to deliver brivanib orally.

Keywords BMS-540215 · Brivanib alaninate · Prodrug · Pharmacokinetics · Oral bioavailability

Introduction

Brivanib alaninate, the L-alanine ester prodrug of brivanib (BMS-540215), an orally available investigational small molecule inhibitor of both vascular endothelial growth factor receptors (VEGFR) and fibroblast growth factor receptors (FGFR), is currently under development for the treatment of cancer, both as a single agent as well as in combination with other cancer treatment modalities [4].

Vascular endothelial growth factor (VEGF) and its corresponding tyrosine kinase receptor (VEGFR) play a critical role in physiological and pathological angiogenesis, a process of forming new capillaries from existing blood vessels. Angiogenesis is essential for solid tumor growth and metastasis [6, 13]. Tumor-induced angiogenesis is mediated by VEGF and several other cytokines, such as

P. H. Marathe (✉) · A. V. Kamath · Y. Zhang · C. D'Arienzo
Pharmaceutical Candidate Optimization, Bristol-Myers Squibb
Pharmaceutical Research Institute, Princeton, NJ 08540, USA
e-mail: punit.marathe@bms.com

R. Bhide
Discovery Chemistry, Bristol-Myers Squibb Pharmaceutical
Research Institute, Princeton, NJ 08540, USA

J. Fargnoli
Biology, Bristol-Myers Squibb Pharmaceutical Research
Institute, Princeton, NJ 08540, USA

platelet-derived growth factor (PDGF) and fibroblast growth factor (FGF), which are secreted by tumor cells. VEGF is known to be the most important angiogenic growth factor in the stimulation of tumor progression [10, 13]. Importantly, the specific binding of VEGF ligand to vascular cell surface-expressed protein kinase receptor VEGFR-2 triggers effective downstream cell proliferation signaling pathways and leads to tumor angiogenesis [12]. The interruption of VEGFR-2 signaling by binding of a small molecule inhibitor to the VEGFR-2 kinase domain has been shown to inhibit angiogenesis, tumor progression and dissemination in a number of preclinical and clinical studies [1]. This approach has been further validated by the recent FDA approval of the antiangiogenic agents including bevacizumab (a monoclonal antibody, which targets the VEGFA ligand) and small molecule inhibitors, sunitinib and sorafenib for the treatment of solid tumors [9, 15–17].

The rationale for the development of brivanib as an anticancer drug stems from the fact that current therapies that are available for patients with advanced metastatic cancer are effective in a minority of eligible patients, the durability of response is usually short-lived, and the toxicities are often dose-limiting. Furthermore, as they are generally administered intravenously, the therapeutic regimens are often inconvenient and invasive. As such, there is a medical need for orally bioavailable, well-tolerated agents that can prolong the life of patients with cancer with minimal safety concerns. Brivanib alaninate represents an orally bioavailable, rationally designed, targeted compound with anticancer activity and acceptable tolerability. In this work, we present preclinical pharmacokinetics, metabolism and in vivo efficacy studies carried out with brivanib alaninate and its parent molecule brivanib to assess suitability for further development.

Materials and methods

Materials

Brivanib alaninate and brivanib were synthesized by discovery chemistry at Bristol-Myers Squibb (BMS). Caco-2 cells (passage # 17) were obtained from the American Type Culture Collection (Rockville, MD). Minimum Essential medium Eagle, nonessential amino acids and Antibiotic-Antimiotic were purchased from JHR Biosciences (Lenexa, KS). Fetal bovine serum was obtained from Hyclone Lab. Inc. (Logan, UT, USA). HTS-Transwell® inserts (surface area: 0.33 cm²) with a polycarbonate membrane (0.4 µm pore size) were purchased from Costar (Cambridge, MA, USA). Hank's balanced salt solution (HBSS) and *N*-2-hydroxyethylpiperazine-*N'*-2-ethanesulfonic acid (HEPES) were purchased from Sigma Chemical Co. (St. Louis, MO,

USA). Mouse and rat hepatocytes were prepared in-house freshly as cell suspensions based on a literature protocol [3]. Fresh dog and monkey hepatocytes were purchased from CEDRA Corporation (Austin, TX, USA). Cryopreserved human hepatocytes were obtained from In Vitro Technologies (Baltimore, MD, USA). All solvents were of analytical grade. All other reagents were of HPLC grade. Millipore Water was used in all experiments.

Sample analysis

Samples obtained from all the pharmacokinetic studies and samples obtained from the protein binding and blood cell partitioning studies were analyzed by LC/MS/MS. Plasma or serum samples were treated with two volumes of acetonitrile containing the internal standard (IS, BMS proprietary compound). After centrifugation to remove precipitated proteins, a 10 µL portion of the clear supernatant was used for analysis. Liver, GI tract, GI contents and brain tissue samples were homogenized on ice with water (1:9) followed by the plasma sample extraction procedure.

Stability experiments were conducted to minimize ex-vivo conversion of brivanib alaninate to brivanib during sample collection, processing and analysis. Based on the results, whole blood samples were collected in tubes containing EDTA and 10% sodium fluoride (2 M) in sodium citrate buffer (0.1 M, pH ~4). All sample processing was done on ice.

The HPLC system consisted of two Shimadzu LC10AD pumps (Columbia, MD, USA), a Shimadzu SIL-HTC auto-sampler (Columbia, MD, USA), and a Hewlett Packard Series 1100 column compartment (Palo Alto, CA, USA). The column was a YMC Pro C18 (2.0 × 50 mm, 3 µm particles) maintained at 60°C and a flow rate of 0.3 mL/min. The mobile phase consisted of 10 mM ammonium formate and 0.1% formic acid in water (A), and 10 mM ammonium formate and 0.1% formic acid in methanol (B). The initial mobile phase composition was 95% A/5% B. After sample injection, the mobile phase composition was changed to 15% A/85% B over 2 min and held at that composition for an additional 1.5 min. The mobile phase was then returned to initial conditions and the column re-equilibrated for 1 min. Total analysis time was 4.5 min. The HPLC was interfaced to a Micromass Quattro LC tandem mass spectrometer equipped with an electrospray ionization source. Ultra-high purity nitrogen was used as the nebulizing and desolvation gas at flow rates of 100 L/h for nebulization and 1,100 L/h for desolvation. The desolvation temperature was 300°C and the source temperature was 150°C. Data acquisition utilized selected reaction monitoring (SRM). Ions representing the (M + H)⁺ species for brivanib, brivanib alaninate and the internal standard were selected in MS1 and collisionally dissociated with argon at a pressure of 2 × 10⁻³ torr to form

specific product ions, which were subsequently monitored by MS2. The parameters for the MS/MS analysis of brivanib, brivanib alaninate and IS were as follows: SRM transition (m/z), 371.3 > 149.1, 442.2 > 130.2 and 529.2 > 91.2, respectively; cone voltage, 30 V for all three compounds; collision energy, 20, 30 and 60 V, respectively; and retention time, 2.8, 2.4 and 2.2 min, respectively.

Stability samples containing plasma, serum, S9, human intestinal microsomes and hepatocytes were analyzed by an LC/MS assay using a Quattro Ultima (Micromass, Manchester, UK) triple quadrupole mass spectrometer interfaced to a Waters 2790 gradient HPLC (Waters Corp., Milford, MA, USA). Samples obtained from the Caco-2 permeability study and glucuronidation assay were analyzed by HPLC-UV. The HPLC system consisted of the 2690 Waters separation module and a Waters 996 photodiode array detector (Waters, Milliford, MA, USA).

For each analytical set, separate standard curves for brivanib alaninate and brivanib were prepared using plasma obtained from whole blood collected on EDTA and 10% sodium fluoride in citrate buffer. The plasma standard curve for brivanib alaninate and brivanib ranged from 1 to 1,000 ng/mL and from 3.9 to 20,000 ng/mL, respectively. The tissue and in vitro standard curves for both compounds ranged from 1 to 10,000 ng/mL. The curves were fitted with a quadratic regression weighted by reciprocal concentration ($1/x$). Standards were analyzed in duplicate. Quality control (QC) samples, prepared in blank plasma, at three concentrations within the range of the calibration curve were also analyzed in triplicate with each plasma analytical set. The predicted concentrations of 80% of the plasma QCs were within 20% of nominal concentration, indicating acceptable assay performance.

Caco-2 permeability

Caco-2 cells were seeded onto 24-well polycarbonate filter membrane at a density of 100,000 cells/cm². Permeability studies were conducted with the monolayers cultured for approximately 21 days in culture, and the cell passage numbers were between 50 and 80. The transport medium buffer was modified Hank's balanced salt solution containing 10 mM HEPES. The pH of both the apical and basolateral compartments was 7.4. The concentration of brivanib alaninate and brivanib used in the P-gp substrate assay was 200 μ M. The bi-directional permeability studies were initiated by adding an appropriate volume of buffer containing brivanib alaninate or brivanib to either the apical (apical-to-basolateral transport) or basolateral (basolateral-to-apical transport) side of the monolayer. Permeability of brivanib alaninate was also assessed in the presence and absence of an esterase inhibitor, PMSF. Samples were taken from both the apical and basolateral

compartment at the end of the 2-h period and the concentrations of test compound were analyzed by HPLC. Permeability coefficient (P_c) was calculated according to the following equation: $P_c = dA/(dt \cdot S \cdot Co)$, where dA/dt is the flux of the compound across the monolayer (nmole/s), S is the surface area of the cell monolayer (0.33 cm²), and Co is the initial concentration (200 μ M) in the donor compartment. The P_c values are expressed in nm/sec.

Serum protein binding and stability

The extent of protein binding of brivanib was determined in fresh mouse, rat, dog and human sera using equilibrium dialysis. All experiments were done in fresh, pooled serum ($n = 10$ for mice, and $n = 3$ for rat, dog and human) obtained from Bioreclamation Inc. (Hicksville, NY, USA). Brivanib (1 mM) in acetonitrile was added into serum at a ratio of 1:100 to give a final concentration of 10 μ M. Serum samples were dialyzed against 134 mM phosphate buffer (pH 7.4). The spiked serum was incubated in a shaking water bath maintained at 37°C for 4 h in a Micro-Equilibrium DialyzerTM (500 μ L chamber volume, Amika Corp., Holliston, MA, USA). A 10,000 dalton molecular weight cutoff dialysis membrane (Amika Corp., Holliston, MA) was used. All experiments were carried out in triplicate. Aliquots of buffer and serum were taken at 4 h and analyzed using the LC/MS/MS method. Serum stability of brivanib was also measured with these serum samples over the 4 h incubation period. Serum stability of brivanib alaninate was investigated in fresh mouse, rat, dog, monkey and human sera in separate experiments.

Blood cell partitioning

The extent of blood cell partitioning of brivanib was determined in mouse, rat, dog, monkey and human blood. All experiments were done in fresh, pooled blood (Bioreclamation Inc., Hicksville, NY). Brivanib (1 mM) in acetonitrile was added into blood at a ratio of 1:100 to give a final concentration of 10 μ M. Samples were incubated at 37°C in a shaking water bath for 2 h. Aliquots of blood were removed at 0.5 and 2 h and the remaining blood was centrifuged to obtain plasma. Blood samples were treated with 0.5 volumes of water and centrifuged to obtain supernatant. All experiments were carried out in triplicate. Blood and plasma samples were analyzed by LC-MS/MS. A blood-to-plasma concentration ratio for brivanib was calculated from the concentrations in blood (C_b) and plasma (C_p).

Microsomal and S9 incubations

The in vitro metabolism of brivanib alaninate was investigated in incubations with S9 subcellular fractions from

mouse, rat, dog, cynomolgus monkey and human liver homogenates and from human intestinal homogenates (Xenotech, Lenexa, KS). The rate of metabolism was measured in duplicate under the following conditions: brivanib alaninate (20 μ M); S9 fractions (20 μ L, 2 mg/mL); in pH 7.4 sodium phosphate buffer (60 mM). Incubations were performed in 96-well plates at 37°C under an atmosphere of 5% CO₂. Incubations were initiated by the addition of S9 and were quenched at various times (0, 10 or 30 min) by the addition of an equal volume (0.2 mL) of acetonitrile to each well. The supernatants were analyzed using an LC/MS assay.

The in vitro metabolism of brivanib alaninate was also investigated in incubations with human intestinal microsomes. The rate of oxidative metabolism was measured in duplicate under the following conditions: brivanib alaninate (10 μ M); intestinal microsomes (1 mg/mL); NADPH (0.9 mg/mL); pH 7.4 sodium phosphate buffer (56 mM). Incubations were performed in 96-well plates at 37°C under an atmosphere of 5% CO₂. Incubations were initiated by the addition of NADPH and were quenched at various times (0, 10 or 30 min) by the addition of an equal volume (0.2 mL) of acetonitrile to each well. Supernatants were analyzed using an LC/MS assay.

Hepatocyte incubations

The metabolic stability of brivanib and brivanib alaninate was evaluated in suspensions of hepatocytes isolated from mouse (CD-1), rat (Sprague-Dawley), dog (beagle), monkey (cynomolgus) and human. The incubations with mouse, rat, dog and monkey hepatocytes were performed with cells from one donor, whereas the incubations with the cryopreserved human hepatocytes were performed with pools from three different donors. Cell viability, determined by trypan blue exclusion, of the fresh hepatocytes was >75% and of the cryopreserved hepatocytes was >60%. Brivanib or brivanib alaninate (3 μ M) was incubated in duplicate at 37°C for 1 h at a cell density of 0.67×10^6 cells/mL in Krebs-Hensleit buffer fortified with glucose, in an incubator at 37°C, with 95% humidity and in an environment of 5% CO₂. Aliquots of samples (0.2 mL) were taken at 0, 20, 40 and 60 min, and the reactions were terminated by adding an equal volume of acetonitrile and analyzed by LC/MS.

Metabolism of brivanib by specific CYP enzymes and FMO3 (reaction phenotyping)

Reaction phenotyping studies were performed for brivanib using SupersomesTM (recombinant singly expressed enzymes) obtained from Gentest Co. (Woburn, MA, USA). Incubations were performed at 37°C using: potassium

phosphate buffer (0.1 M, pH 7.4) containing NADPH (1 mM), magnesium chloride (3.3 mM), CYP450 supersomes (100 pmol/mL) or FMO3 (0.5 mg/mL), vector protein and brivanib (1, 10 or 100 μ M). After a 5 min pre-incubation at 37°C, the reaction was initiated by the addition of NADPH: the final incubation volume was 1 mL. After 0 and 30 min, the incubation was vortex-mixed; triplicate aliquots were taken and quenched with twice the volume of acetonitrile. Samples were analyzed using LC/MS/MS.

In vivo pharmacokinetic studies

All animal studies were performed under the approval of the Bristol-Myers Squibb Animal Care and Use Committee and in accordance with the American Association for Accreditation of Laboratory Animal Care.

Mouse

The pharmacokinetics of brivanib was investigated in male balb-c mice. A total of 18 mice were divided into two groups to receive brivanib as a single dose of 10 mg/kg IV or 60 mg/kg orally by gavage. The exposure of brivanib after administration of the prodrug brivanib alaninate was also investigated after a single oral dose (30 mg/kg) to a group of nine male balb-c mice. The vehicle used was PEG400:water (1:1) for the IV dose and PEG400:tween 80 (75:25) for the oral dose of brivanib. The vehicle used for brivanib alaninate dosing was sodium acetate buffer (50 mM, pH 4.6). Serum concentrations of brivanib and brivanib alaninate were measured at 3 and 30 min, and 1, 3, 6, 8 and 24 h after IV dosing and at 30 min, and 3, 8 and 24 h after oral dosing. The mice were fasted overnight and fed 6 h after dosing. Three blood samples were taken from each mouse and there were three mice per time point. At the 24 h time point, only one sample was taken from each of the three mice. Blood samples taken after brivanib alaninate administration were stabilized by the addition of 10% sodium fluoride (2 M) in sodium citrate buffer (0.1 M), pH ~4, added to prevent any ex vivo conversion of brivanib alaninate to brivanib. Composite serum concentration–time profiles were constructed for pharmacokinetic analysis.

Rat

Brivanib was administered to male Sprague-Dawley rats as a 10 min infusion intraarterially (IA) (10 mg/kg) or orally by gavage (25 mg/kg) ($n = 3$). The dosing vehicle used was PEG400:ethanol:water (70:10:20). In another study, the oral exposure of brivanib was investigated using three different oral formulations at three dose levels (25, 100 and 200 mg/kg). Formulation #1 was PEG400:tween 80 (75:25).

Formulation #2 was a micronized suspension in 0.1% tween 80 (average particle size $\sim 7.1\ \mu\text{m}$, 95% of the particles sized less than $17\ \mu\text{m}$). Formulation #3 was a nanosuspension in hydroxypropyl cellulose (0.25–2%) and sodium lauryl sulfate (0.002–0.02%) (95% of the particles sized less than $209\ \text{nm}$). The exposure of brivanib after administration of brivanib alaninate was investigated following single doses of 50, 200 or 360 mg/kg orally by gavage. The dosing vehicle used was 50 mM sodium acetate buffer, pH 4.6. In all studies, the rats were fasted overnight and fed 4 h post-dose. Blood samples were collected at 15, 30 and 45 min, and 1, 2, 4, 6, 8, 10, 24 and 48 h after IA and oral dosing. An additional 10 min sample was collected after IA dosing. Approximately, 0.3 mL of blood was collected from the jugular vein in tubes containing EDTA, and plasma was obtained by centrifugation. Samples collected after brivanib alaninate dosing were stabilized by the addition of $\sim 300\ \mu\text{L}$ sodium fluoride solution (2 M) in sodium citrate buffer (0.1 M, pH ~ 4). Samples were analyzed for brivanib and brivanib alaninate by LC/MS/MS.

The brain uptake of brivanib alaninate and brivanib was investigated after a single oral dose of brivanib alaninate (120 mg/kg). Brain tissues and blood samples were collected at 1, 4, 10 and 24 h post-dose. Plasma and tissue samples were analyzed for brivanib and brivanib alaninate by LC/MS/MS.

Dog

The pharmacokinetics of brivanib was investigated in male beagle dogs ($n = 3$) following a 10 min IV infusion (1 mg/kg) and an oral dose (4.5 mg/kg) by gavage in a cross-over study design. The vehicle used for the IV route was PEG300:5% dextrose in water (6:4) and the vehicle for the oral dose was 100% PEG400. The exposure of brivanib after administration of brivanib alaninate was investigated following single oral doses of 4.5, 30 and 100 mg/kg by gavage ($n = 2$). The vehicle used was 50 mM sodium acetate buffer, pH 4.6. The dogs were fasted overnight and fed 4 h post-dose. Blood samples were collected at 10, 15, 30 and 45 min, and 1, 2, 4, 6, 8, 10 and 24 h after IV and oral dosing. Approximately, 1 mL of blood was collected in tubes containing EDTA and plasma was obtained by centrifugation. Blood samples collected after brivanib alaninate dosing were stabilized by the addition of 10% sodium fluoride (2 M) in sodium citrate buffer (0.1 M, pH ~ 4). Urine was collected over a 24 h period. Samples were stored at -20°C until analysis by LC/MS/MS.

Monkey

For the pharmacokinetic investigation in male cynomolgus monkeys, brivanib was infused IV for 10 min (1 mg/kg) or

administered as an oral solution (5 mg/kg) by gavage, in a cross-over study design. The vehicle used for both the IV and oral routes was PEG400:water (6:4). The exposure of brivanib after administration of brivanib alaninate was determined following single doses of 5, 30 or 60 mg/kg orally by gavage. The vehicle used was 50 mM sodium acetate buffer, pH 4.5. The monkeys were fasted overnight and fed 4 h post-dose. Blood samples were collected at 10, 15, 30 and 45 min, and 1, 2, 4, 6, 8, 10 and 24 h after IV and oral dosing. Approximately, 1 mL of blood was collected in tubes containing EDTA and plasma was obtained by centrifugation. Blood samples collected after brivanib alaninate dosing were additionally stabilized with a 10% sodium fluoride solution (2 M) in sodium citrate buffer (0.1 M, pH ~ 4). Samples were stored at -20°C until analysis by LC/MS/MS.

Efficacy studies in nude mice

L-2987 human lung and HCT-116/VM46 human colon tumors were maintained by serial subcutaneous passage in athymic (nu/nu) 5–6 week-old female balb/c mice purchased from Harlan Sprague Dawley (Indianapolis, IN, USA). The animals were maintained in an ammonia and pathogen-free environment and fed water and food ad libitum. Mice were maintained in quarantine for 7 days prior to tumor implantation and efficacy testing. Tumors were implanted subcutaneously as small fragments, generally no larger than $0.1\text{--}0.2\ \text{mm}^3$ using a 16 g trocar. All tumors that were evaluated were allowed to grow to an approximate size of $100\text{--}125\ \text{mm}^3$ prior to the initiation of treatment. The treatment and control group sizes consisted of 8–10 mice. The tumor size was measured twice weekly. Tumor volume was calculated by measuring perpendicular tumor diameters using Vernier scale calipers and using the formula: $1/2 (\text{length} \times (\text{width})^2)$. Blood was obtained from mice for pharmacokinetic analysis over 24 h post-last dose by retro-orbital sinus bleeding in accordance with institutional policy. Serum was separated by centrifugation and analyzed by LC-MS/MS.

The vehicles used for brivanib alaninate and brivanib were sodium citrate buffer (pH 4.6) and PEG400:water (7:3), respectively (0.01 mL/g body weight). Both compounds were dosed orally using disposable 20 g oral gavage needles (Popper and Sons, Inc., New Hyde Park, NY, USA) on a daily schedule with a general duration of 9–14 days. An active response was determined by $T/C \leq 0.42$ where T is the median tumor size in treated mice and C is the median tumor size in vehicle-treated mice [7].

Pharmacokinetic data analysis

Plasma concentration versus time data of brivanib and brivanib alaninate were analyzed by noncompartmental

methods [14] using the KINETICATM software program. The C_{\max} and T_{\max} values were recorded directly from experimental observations. The AUC_{0-n} and AUC_{tot} values were calculated using a combination of linear and log trapezoidal summations. The total body clearance (CL), mean residence time (MRT), and the steady state volume of distribution (V_{ss}) of brivanib were also calculated after IV administration of brivanib. The absolute oral bioavailability of brivanib (expressed as %) on administration of brivanib was estimated by taking the ratio of dose-normalized AUC values after oral doses to those after intravenous doses. The apparent oral bioavailability of brivanib on administration of the prodrug brivanib alaninate was estimated by taking the ratio of dose-normalized AUC values of brivanib after an oral dose of brivanib alaninate to those after an IV dose of brivanib.

The in vitro intrinsic clearance of brivanib in hepatocytes (CL_{int}) was calculated as CL_{int} (mL/min per million cells) = rate/ C , where rate is the rate of metabolism in hepatocytes (pmole/min per million cells), and C is the concentration of brivanib in the incubation. The in vivo intrinsic hepatic clearance of brivanib ($CL_{\text{h, in vivo}}$) estimated from in vitro hepatocyte incubations was calculated as follows:

$$CL_{\text{h, in vivo}} = (CL_{\text{int}}) \times \left(\frac{120 \times 10^6 \text{ cells}}{1 \text{ g liver weight}} \right) \times \left(\frac{\chi \text{ g of liver weight}}{\text{kg of body weight}} \right)$$

where χ is 88, 40, 32, 32 and 21 g liver/kg body weight for the mouse, rat, dog, monkey and human, respectively [8]. Protein binding in the incubation mixture or plasma was not factored into these calculations. The hepatic clearance (CL_h) was calculated from the following equation using the well-stirred model:

$$CL_{\text{h}} = \frac{Q_{\text{h}} \times CL_{\text{int}}}{Q_{\text{h}} + CL_{\text{int}}}$$

Where, Q_{h} is the liver blood flow of 90, 55, 31, 44 and 21 mL/min per kg for the mouse, rat, dog, monkey and human, respectively [8]. Hepatic extraction ratio was calculated by dividing the predicted or observed CL by the hepatic blood flow for that species.

Results

Permeability studies using Caco-2 cells

The permeability coefficient (P_c) of brivanib in the apical-to-basolateral (A-to-B) direction was 204 nm/s at an initial concentration of 200 μM (pH 7.4). The permeability of brivanib is comparable to compounds that exhibit good

absorption (>50%) in humans. Permeability of brivanib alaninate in Caco-2 cells could not be determined due to its rapid hydrolysis to brivanib. Within 15 min of adding brivanib alaninate to the Caco-2 cells, brivanib was seen on both the donor and receiver side of the Caco-2 cells. Addition of PMSF, an esterase inhibitor, did not prevent this hydrolysis. This conversion of brivanib alaninate to brivanib in Caco-2 cells with the appearance of brivanib on the receiver side suggests good permeability, which should translate into good absorption of brivanib in humans when administered as brivanib alaninate.

The basolateral-to-apical (B-to-A) Caco-2 cell monolayer permeability of brivanib was measured in order to determine if the compound was a P-gp substrate. The average B-to-A P_c value of brivanib was 112 nm/s at an initial concentration of 200 μM (pH 7.4), suggesting that brivanib is not a P-gp substrate.

Serum stability and protein binding

Brivanib was stable in mouse, rat, dog and human serum for 4 h at 37°C. The serum protein binding of brivanib was found to be 98, 99.8, 98.2 and 98.7% in mouse, rat, dog and human, respectively.

The stability of brivanib alaninate was determined in serum and plasma from mouse, rat, dog, monkey and human. The half life of brivanib alaninate in serum was found to be 11, 19 and 75 min in mouse, rat and monkey, respectively, and greater than 180 min in dog and human. The half life of brivanib alaninate in plasma was less than 10 min in mouse and rat, 141 min in monkey, 158 min in dog and greater than 200 min in human. In both serum and plasma, brivanib alaninate was hydrolyzed to brivanib suggesting that brivanib alaninate is highly unstable in mouse and rat serum/plasma, but relatively stable in dog, monkey and human serum/plasma.

Microsomal, S9 and hepatocyte stability

The rate of metabolism of brivanib in hepatocytes predicts low clearance in the mouse, high clearance in the rat and intermediate clearance in dog, monkey and human (Table 1). There was no turnover of brivanib in mouse hepatocytes. Predicted in vivo CL from rat, dog and monkey hepatocytes was approximately two to threefold higher than the observed systemic CL in these species. This suggests that brivanib is likely to have low to moderate CL (hepatic extraction ratio <0.7) in the human.

The stability of brivanib alaninate was determined in liver S9 fractions from mouse, rat, dog, monkey and human. Brivanib alaninate was hydrolyzed to brivanib in all species with a half life of less than 10 min. Brivanib alaninate was also found to be rapidly hydrolyzed to

Table 1 Rates of oxidative metabolism of brivanib in hepatocytes and predicted in vivo hepatic clearances

Species	Hepatocytes		In vivo blood CL (observed) (ml/min per kg)
	Rate (pmol/min per 10 ⁶ cells)	Predicted CL (ml/min per kg)	
Mouse	0	0 (0)	13.7 (0.15)
Rat	150	54 (0.98)	31 (0.56)
Dog	35	20 (0.65)	8.8 (0.28)
Monkey	45	25 (0.57)	8.6 (0.20)
Human	41	13 (0.62)	–

Hepatic extraction ratio is in parenthesis

brivanib in human intestinal S9 and microsomes with a half life of less than 10 min. Brivanib alaninate was rapidly metabolized in hepatocytes from all species, with complete disappearance within 20 min of incubation. These results suggest efficient conversion of brivanib alaninate to brivanib in liver and intestinal fractions in all species.

Reaction phenotyping

Brivanib appears to be primarily metabolized by CYP3A4 based on the turnover in recombinant single-enzyme test systems, and their relative expression in the human liver. Many enzymes appeared capable of metabolizing brivanib, including CYP3A4, 3A5, 1A1, 2C19, 2E1, 2B1 and FMO3 (Table 2). Some of these enzymes are expressed extra-hepatically and may contribute to the total metabolic clearance. The known relative expression of CYPs in human liver would indicate CYP3A4 to be the primary metabolic pathway, possibly switching to a low-affinity CYP3A5 component at higher concentrations. Nevertheless, the turnover of brivanib by CYP3A4 was low, suggesting that in vivo CL of brivanib will be low.

Pharmacokinetics in mice

The systemic serum clearance of brivanib in mice was 9.3 mL/min per kg, which is equivalent to a blood clearance of 13.7 mL/min per kg (Table 3) based on a blood to plasma concentration ratio of 0.75. The blood clearance of brivanib is ~15% of the hepatic blood flow in mice [8]. The steady state volume of distribution was high (2 L/kg), greater than the blood volume of 0.085 L/kg, indicating significant extravascular distribution. The estimated half life was 2.7 h and the mean residence time (MRT) was 3.6 h. The oral bioavailability of brivanib in mice was 88% at 60 mg/kg. When administered as brivanib alaninate, the apparent oral bioavailability of brivanib was estimated to be ~80% (Table 4). Serum concentrations of brivanib alaninate were <LLQ (1 ng/mL).

Pharmacokinetics in rats

The systemic plasma clearance of brivanib was 21.4 mL/min per kg (equivalent to a blood clearance of 31 mL/min per kg based on the blood-to-plasma concentration ratio of 0.61) (Table 3). The blood clearance of brivanib is ~56% of the hepatic blood flow in rats. The steady state volume of distribution was moderate (0.94 L/kg), greater than the blood volume of 0.054 L/kg, indicating extravascular distribution. The estimated elimination half life was 1.0 h and the mean residence time was 0.75 h. The oral bioavailability of brivanib was 25% at the 25 mg/kg dose. The time to reach peak concentrations (T_{max}) after an oral dose was 0.5 h in the rat. The oral exposure of brivanib was evaluated using three different formulations (PEG400:tween 80 solution (75:25), micronized suspension and nanosuspension), at three dose levels (25, 100 and 200 mg/kg) (Table 5). Both micronized and nanosuspensions provided poor exposures at all doses. The exposures observed with the PEG400:tween-80 formulations, though not dose proportional, were much higher than the micronized and nanosuspensions. However, due to the large amount of tween-80 needed, this formulation was deemed unsuitable for further development.

When brivanib alaninate was orally administered to rats (50, 200 and 360 mg/kg) (Table 6), plasma concentrations of brivanib alaninate were less than the LLQ (1 ng/mL). The AUC_{tot} of brivanib increased in a dose-proportional manner. The apparent oral bioavailability of brivanib after administration of brivanib alaninate was estimated to be ~55% at the 50 mg/kg dose. Of particular note is the fact that the apparent oral bioavailability of brivanib did not decrease up to a dose of 360 mg/kg when dosed as brivanib alaninate in a completely aqueous vehicle. The extent of brain penetration of brivanib was determined in rats after a single oral dose of brivanib alaninate (120 mg/kg). The plasma and brain concentrations of brivanib alaninate were <LLQ for all rats. The brain to plasma ratio for brivanib was ~1.7, based on AUC_{0-24} , indicating significant distribution into the brain in rats.

Pharmacokinetics in dogs

The systemic plasma clearance of brivanib was 5.8 ± 1.0 mL/min per kg, equivalent to a blood clearance of 8.8 mL/min per kg based on the blood-to-plasma concentration ratio of 0.57 (Table 3). The blood clearance of brivanib is ~28% of the hepatic blood flow in dogs. The steady state volume of distribution was moderate (0.9 ± 0.3 L/kg), greater than blood volume of 0.09 L/kg, indicating extravascular distribution. The estimated elimination half life was 2.8 ± 1.3 h and the mean residence time was 2.6 ± 0.8 h. The oral bioavailability of brivanib was

Table 2 Rates of oxidative metabolism of brivanib by cDNA-expressed human CYPs and FMO3 (reaction phenotyping)

Enzyme	Rate of metabolism, pmol/min per pmol CYP (% turnover in 30 min)		
	1 μ M	10 μ M	100 μ M
1A1	0.344 (52)	1.005 (15)	3.469 (5.2)
1A2	0.048 (7.1)	0.344 (5.2)	2.353 (3.5)
2A6	0.057 (8.6)	0.220 (3.3)	6.386 (9.6)
2C9	0.000 (−1.2)	0.000 (−1.8)	4.333 (6.5)
2C19	0.093 (14)	0.000 (−1.9)	2.801 (4.2)
2D6	0.006 (1)	0.409 (6.1)	2.096 (3.1)
2E1	0.129 (19)	0.961 (14)	9.062 (14)
3A4	0.148 (22)	1.595 (24)	6.518 (9.8)
FMO3 ^a	27.08 (20)	132 (9.9)	1258 (9.4)
2C8	0.027 (4)	0.000 (−1.5)	5.180 (7.8)
3A5	0.053 (8)	0.911 (14)	21.269 (32)
1B1	0.148 (22)	0.253 (3.8)	7.289 (11)
2B6	0.028 (4.2)	0.471 (7.1)	3.313 (5.0)
4A11	0.000 (−0.3)	0.290 (4.4)	6.329 (9.5)

^a Units for FMO3 are pmol/min per mg protein

Table 3 Pharmacokinetics of brivanib in animals following administration of brivanib

Species	Route	Dose (mg/kg)	C_{\max} (μ g/mL)	T_{\max} (h)	AUC_{tot}^a (μ g h/mL)	$t_{1/2}$ (h)	CL (mL/min per kg)	V_{SS} (L/kg)	F (%)
Mouse ^b	IV	10	–	–	15.8	2.7	9.3	2.0	–
	PO	60	17.8	1	83	–	–	–	88
Rat ^c	IA	10	–	–	7.9	1.02	21.4	0.94	–
	PO	25	2.4 ± 1.07	0.5 ± 0.0	4.96 ± 1.7	–	–	–	25
Dog ^d	IV	1	–	–	2.9 ± 0.53	2.8 ± 1.3	5.8 ± 1.0	0.9 ± 0.3	–
	PO	4.5	0.56 ± 0.34	1 ± 0.0	2.8 ± 2.8	–	–	–	22 ± 22
Monkey ^e	IV	1	–	–	2.9 ± 0.78	3.3 ± 1.3	6.0 ± 1.7	1.5 ± 0.7	–
	PO	5	1.5 ± 0.59	1.3 ± 0.7	10 ± 0.48	–	–	–	68 ± 14

^a AUC_{0-8} reported for the mouse

^b Dosing vehicle: IV-PEG400:water (60:40), PO-PEG400:tween80 (75:25)

^c Dosing vehicle: IV and PO-PEG400:ethanol:water (70:10:20)

^d Dosing vehicle: IV-PEG300:5% dextrose in water (60:40), PO-PEG400 (100%)

^e Dosing vehicle: IV and PO-PEG400:water (60:40)

Table 4 Systemic exposure of brivanib in animals following administration of brivanib alaninate

Species ^a	Route	Dose (mg/kg)	C_{\max} (μ g/mL)	T_{\max} (h)	AUC_{tot}^b (μ g h/mL)	F (%)
Mouse	PO	30	6.1	0.5	36.7	80
Rat	PO	50	6.7 ± 2.3	1.3 ± 0.6	18.3 ± 2.2	55
Dog	PO	4.5	1.4	0.6	5.7	52
Monkey	PO	5	2.5 ± 0.78	1.3 ± 0.7	12 ± 1.04	97

^a Dosing vehicle was 50 mM sodium acetate buffer, pH 4.6

^b AUC_{0-24} reported for the monkey

$22 \pm 22\%$ when dosed in a 100% PEG400 formulation. The time to reach peak concentrations (T_{\max}) after an oral dose was 1 h in the dog. Brivanib was not detected in the urine over a 24 h period after both the IV and oral doses.

Similar to the observation in mice and rats, plasma concentrations of brivanib alaninate were less than LLQ (1 ng/mL) after the 4.5 mg/kg oral dose (Table 4, Fig. 1). At the 30 mg/kg oral dose, brivanib was detectable up to 15 min at concentrations of <4.4 ng/mL. The apparent oral

Table 5 Systemic exposure of brivanib in rats after oral administration of brivanib using three different formulations

Formulation	Dose (mg/kg)	Parameter ($n = 3$)		
		C_{\max} ($\mu\text{g/mL}$)	T_{\max} (h)	AUC_{tot} ($\mu\text{g h/mL}$)
PEG400:tween 80 (75:25)	25	4.0 ± 1.7	2.3 ± 2.0	6.9 ± 3.6
	100	22.2 ± 11.7	9.1 ± 8.4	163 ± 97
	200	26.7 ± 11.7	3.4 ± 0.1	199 ± 64
Micronized suspension (0.1% tween 80)	25	0.20 ± 0.03	4.7 ± 1.2	1.2 ± 0.24
	100	0.76 ± 0.19	4.0 ± 0.0	3.1 ± 0.55
	200	0.63 ± 0.20	4.0 ± 0.0	2.8 ± 0.76
Nanosuspension	25	1.1 ± 0.18	2.0 ± 0.0	4.4 ± 0.55
	100	2.7 ± 0.95	2.0 ± 0.0	12.3 ± 3.5
	200	2.8 ± 0.81	2.7 ± 1.2	12.9 ± 2.7

Table 6 Systemic exposure of brivanib in rats after administration of brivanib alaninate

Dose (mg/kg)	C_{\max} ($\mu\text{g/mL}$)	T_{\max} (h)	AUC_{tot} ($\mu\text{g h/mL}$)
50	6.7 ± 2.3	1.3 ± 0.6	18.3 ± 2.2
200	13 ± 2.2	0.9 ± 0.1	73 ± 11
360	15 ± 1.6	0.8 ± 0.1	133 ± 25

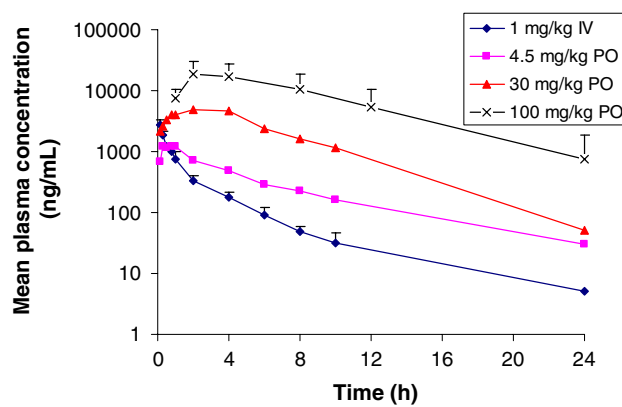
Vehicle: 50 mM sodium acetate buffer, pH 4.6

bioavailability of brivanib after administration of brivanib alaninate was estimated to be $\sim 52\%$ at the 4.5 mg/kg dose. The systemic exposure to brivanib (AUC_{tot}) after oral administration of brivanib alaninate increased with dose as high as 100 mg/kg and administered in a completely aqueous vehicle.

Pharmacokinetics in monkeys

In monkeys, after an IV dose of brivanib (1 mg/kg), the systemic plasma clearance was 6.0 ± 1.7 mL/min per kg (Table 3), equivalent to a blood clearance of 8.8 mL/min per kg (assuming a blood to plasma concentration ratio of 0.68). The blood clearance of brivanib is $\sim 20\%$ of the hepatic blood flow. The steady state volume of distribution was moderate (1.5 ± 0.7 L/kg), greater than the blood volume of 0.073 L/kg, indicating extravascular distribution. The estimated elimination half life was 3.3 ± 1.3 h and the mean residence time was 3.9 ± 0.8 h. The oral bioavailability of brivanib was $68 \pm 14\%$ at a 5 mg/kg oral dose. The time to reach peak concentrations (T_{\max}) after an oral dose was 1.3 ± 0.7 h in the monkey.

Plasma concentrations of brivanib alaninate were less than the LLQ (1 ng/mL) after oral administration of brivanib alaninate. The systemic exposure to brivanib (AUC_{0-24}) increased in a greater than dose-proportional manner from 5 to 60 mg/kg. At the 30 and 60 mg/kg oral dose, plasma concentrations of brivanib remained elevated

**Fig. 1** Plasma concentration versus time profiles of brivanib after IV administration of brivanib and oral administration of brivanib alaninate in dogs (IV dose: 1 mg/kg, PO doses: 4.5, 30, 100 mg/kg)

up to 24 h. The apparent oral bioavailability of brivanib after administration of brivanib alaninate was estimated to be $\sim 97\%$ at the 5 mg/kg dose. The oral bioavailability showed a significant improvement when brivanib was administered as its prodrug in a completely aqueous vehicle (Table 4, Fig. 2).

Efficacy in nude mice bearing human xenografts

Brivanib was initially evaluated for in vivo antitumor activity in the L2987 human lung solid tumor xenograft model at three dose levels. As demonstrated in Fig. 3, when brivanib was dosed orally on a once-a-day schedule for 9 days, tumor growth delay was observed at 60 and 90 mg/kg with the respective T/C values of 0.40 and 0.36 at day 9. No weight loss or overt toxicity was observed at any of these dose levels. Brivanib alaninate was at least as active as brivanib (at equimolar doses) in delaying tumor growth (Fig. 4) with T/C values of 0.31 (at 66 mg/kg per day equivalent of brivanib) and 0.27 (at 90 mg/kg per day equivalent of brivanib), respectively, on day 14. T/C values

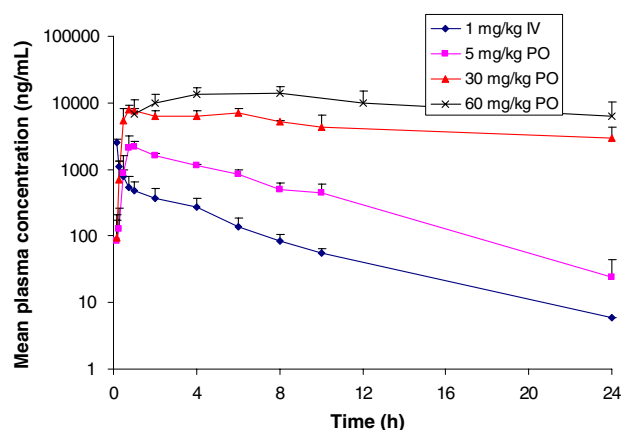


Fig. 2 Plasma concentration versus time profiles of brivanib after IV administration of brivanib and oral administration of brivanib alaninate in monkeys (IV dose: 1 mg/kg, PO doses: 5, 30, 60 mg/kg)

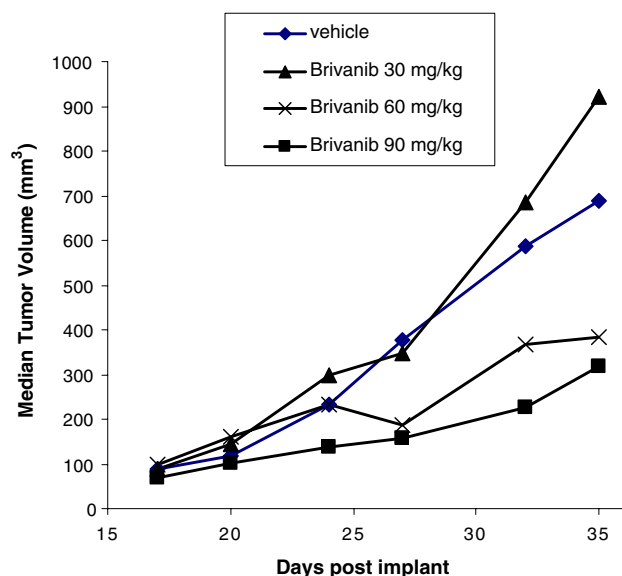


Fig. 3 Antitumor efficacy of brivanib in L2987 human lung carcinoma administered on a q1d × 9 schedule (doses: vehicle, 30, 60 and 90 mg/kg per day)

at 9 days of dosing with brivanib alaninate were similar, although not identical. Consistent with complete conversion of brivanib alaninate to brivanib, pharmacokinetic analysis demonstrated comparable exposure levels of brivanib, following oral dosing of brivanib alaninate (data not shown) with no quantifiable levels of brivanib.

Brivanib alaninate was also evaluated in the HCT116/VM46 human colon tumor xenograft model, a tumor cell line with resistance to multiple chemotherapeutic agents due to P-gp overexpression [18]. As shown in Fig. 4, a dose of 60 mg/kg per day of brivanib alaninate (equivalent to 50 mg/kg of brivanib) was active with a *T/C* of 0.39, similar to the antitumor activity observed in L2987. Similar

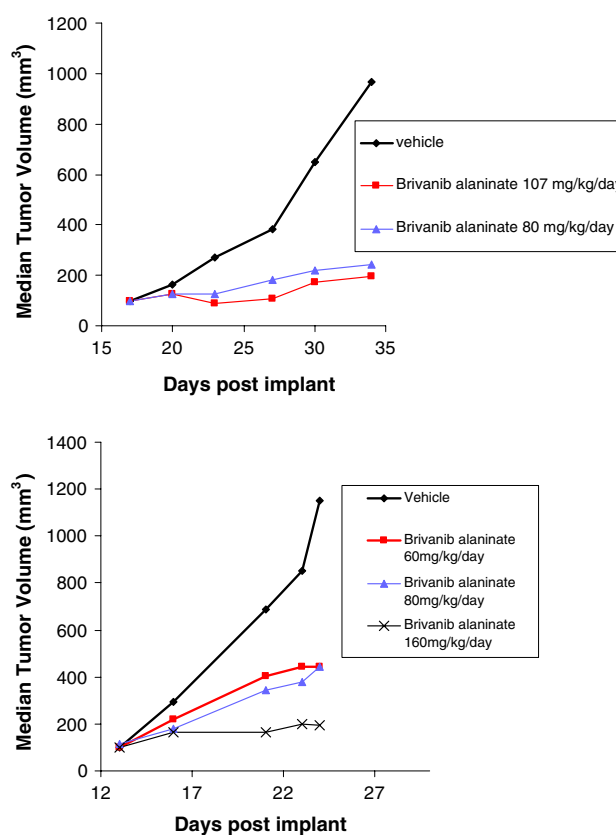


Fig. 4 Upper panel: antitumor efficacy of brivanib alaninate in L2987 human lung carcinoma administered on a q1d × 9 schedule (doses: vehicle, 80 and 107 mg/kg per day). Lower panel: antitumor efficacy of brivanib alaninate in HCT116/VM46 human colon carcinoma administered on a q1d × 12 schedule (doses: vehicle, 60, 80, 160 mg/kg per day)

antitumor activity was observed at the mid-dose (80 mg/kg per day brivanib alaninate). A higher dose of brivanib alaninate (160 mg/kg per day, equivalent to 133 mg/kg per day of brivanib) was highly active with a *T/C* of 0.17. The minimum efficacious dose was 60 mg/kg with a measured exposure (AUC_{0-24} at steady state) of 33.7 $\mu\text{g h/ml}$. Thus, brivanib alaninate is active in vivo against a tumor line highly resistant to chemotherapeutic agents, presumably due to the targeting of the endothelial cell host compartment, consistent with its anti-angiogenic effect.

Prediction of human CL and efficacious dose

The systemic CL of brivanib was assumed to be all hepatic, consistent with <0.1% of unchanged brivanib in the rat and dog (data not shown). The observed systemic CL in the mouse, rat, dog and monkey was converted to CL_{int} in vivo and compared to the predicted CL_{int} from hepatocytes. Since there was no turnover of brivanib in the presence of mouse hepatocytes, the mouse was excluded from this analysis. Based on the correlation of predicted and

observed CL_{int} , in vivo in the rat, dog and monkey, the CL_{int} , in vivo in the human was predicted to be 7.3 mL/min per kg, which translated to a systemic CL of 5.3 mL/min per kg.

The steady state exposure of brivanib at the minimum efficacious dose (administered as brivanib alaninate) in nude mice bearing HCT116/VM46 human xenograft was 33.7 μ g h/mL. Based on this exposure, the predicted human systemic CL and an average apparent oral bioavailability of 71% in four nonclinical species, the minimum efficacious dose of brivanib alaninate was predicted to be 18 mg/kg per day (1.3 g total).

Discussion

Brivanib was found to be a low CL compound with a large volume of distribution and adequate half life in all four nonclinical species tested. The Caco-2 permeability studies suggested that brivanib should have adequate permeability for absorption through the GI tract. The predicted human CL based on human hepatocytes was also in the low to moderate range. Despite these properties, the predicted human efficacious dose was relatively high (1.3 g). Oral administration of brivanib in rat (at 25 mg/kg) as a micronized suspension produced significantly lower (~fivefold) systemic exposure of brivanib than those obtained from solution formulations. The low aqueous solubility (<1 μ g/mL at pH 6.5) of brivanib presumably contributed to dissolution rate-limited absorption of the compound, particularly at high doses. Efforts to improve the oral bioavailability and increase drug plasma concentrations of brivanib at high doses (>100 mg/kg) using different early formulation strategies (a solubilized system, a micronized system, and a nanosized system) were unsuccessful.

When dosed as brivanib, the oral bioavailability was 88, 25, 22 and 68% in mice, rats, dogs and monkeys, respectively. However, due to poor solubility, dissolution-limited absorption of brivanib was seen, with less than dose-proportional increase in exposure, which prevented attaining adequate multiples of exposure for toxicity evaluation with brivanib. Additionally, in higher species (dog), the amount of excipients (PEG alone or with Tween-80) could have caused GI toxicity at the volumes needed to solubilize brivanib. It was also deemed difficult to achieve adequate exposures in the clinic with traditional formulation technologies. A soluble prodrug strategy was explored as an alternative means to enable the development of brivanib [5].

Most technologies employed to deliver poorly soluble compounds have the liability of a low drug load. Therefore, these technologies are most useful when paired with a drug candidate with a low dose. To increase the solubility of

brivanib, a prodrug approach was investigated. A prodrug with increased solubility, stability at the gastric pH, and the ability to cleave in plasma may enable exposures needed to advance the project in toxicological studies and move quickly toward proof of concept in humans.

Prodrug technology over the last several years has made great advances largely based on the application of creative technology that has been developed for linking a drug to a pro-moiety via a cleavable element that facilitates optimal drug release kinetics [20, 21]. Typically, useful elements that can be derivatized directly with a prodrug moiety include alcohols, amines and carboxylic acids, while sterically hindered alcohols and amines, amides, imides and heterocycles will usually require the incorporation of linker technology. Brivanib offers an easy handle for prodrug formation in the form of a secondary alcohol functionality. Amino acid ester prodrugs of alcohols have been used successfully in marketed drugs to improve aqueous solubility [2]. Enzymatic release can occur pre-systemically or systemically after absorption of the prodrug. Clearly, pre-systemic cleavage will minimize exposure to the prodrug, a consideration of potential importance from a toxicological perspective [22].

In case of brivanib alaninate, the cleavage of the alanine ester functionality appears to occur pre-systemically. Brivanib alaninate was found to be unstable in rodent plasma and serum consistent with high concentration of nonspecific esterases, but was relatively stable in dog, monkey and human plasma [19]. Stability in human plasma raised a concern that brivanib alaninate may circulate in sufficiently high concentrations in human plasma making its safety evaluation difficult based on rodent studies. Efforts were then carried out to investigate the stability of brivanib alaninate in human-derived liver and intestinal microsomes and S9. Brivanib alaninate was found to cleave rapidly to brivanib in these matrices, suggesting that there would not be significant circulating concentrations of the prodrug in human plasma. In addition, no circulating concentrations of brivanib alaninate were detected in mouse, rat and monkey plasma after oral doses of brivanib alaninate except in the dog at 30 mg/kg where <4.4 ng/mL concentrations of brivanib alaninate were found up to 15 min post-dose.

The rapid and complete pre-systemic cleavage of brivanib alaninate to brivanib was supported by the improvement in the apparent oral bioavailability of brivanib when dosed as the prodrug (80, 55, 52 and 97% in mice, rats, dogs and monkeys, respectively). In addition, dose-proportional or greater than dose-proportional increases in exposures to brivanib with increasing dose of brivanib alaninate were seen in animal species at doses up to 360 mg/kg. Antitumor efficacy was demonstrated with equimolar doses of brivanib alaninate and brivanib in nude mice bearing L2987 human lung and HCT116/VM46 human colon carcinomas with a

minimum efficacious dose of 60 mg/kg per day of brivanib alaninate and an associated exposure of 33.7 $\mu\text{g}\cdot\text{h}/\text{mL}$ measured as brivanib. In clinical trials with cancer patients, pharmacodynamic response (DCE-MRI, collagen IV) was observed at the maximum tolerated dose (800 mg QD) and the associated average exposure was 60 $\mu\text{g}\cdot\text{h}/\text{mL}$ [11]. Based on this observation, a brivanib alaninate dose of 800 mg QD is recommended for future clinical trials. The preclinical pharmacokinetics and efficacy studies with brivanib alaninate successfully predicted the human efficacious dose within twofold.

In conclusion, brivanib shows low to intermediate clearance in mouse, rat, dog and monkey, and distributes extensively in those species. The prodrug, brivanib alaninate, is rapidly and efficiently converted to the parent, brivanib, as demonstrated both in vitro and in vivo and offers an excellent mode to deliver brivanib orally. Overall, the preclinical investigation of the pharmacokinetics and in vivo efficacy of brivanib and its prodrug brivanib alaninate demonstrates its utility to project human pharmacokinetics and efficacious doses.

Acknowledgments We would like to thank Anthony Marino and Melissa Yarde for conducting the Caco-2 experiments, George Derbin for formulation support, Carl Davies for reaction phenotyping studies, and R. M. Fancher and the technical services unit for their help with all in vivo studies.

References

- Baka S, Clamp AR, Jayson GC (2006) A review of the latest clinical compounds to inhibit VEGF in pathological angiogenesis. *Expert Opin Ther Targets* 10:867–876
- Beaumont K, Webster R, Gardner I, Dack K (2003) Design of ester prodrugs to enhance oral absorption of poorly permeable compounds: challenges to the discovery scientist. *Curr Drug Metab* 4:461–485
- Berry M, Edwards AM, Barritt GJ (1991) Isolated hepatocytes preparation, properties and applications in laboratory techniques in biochemistry and molecular biology. Elsevier, Amsterdam
- Bhide RS, Cai ZW, Zhang YZ, Qian L, Wei D, Barbosa S, Lombardo LJ, Borzilleri RM, Zheng X, Wu LI, Barrish JC, Kim SH, Leavitt K, Mathur A, Leith L, Chao S, Wautlet B, Mortillo S, Jayaseelan R Sr, Kukral D, Hunt JT, Kamath A, Fura A, Vyas V, Marathe P, D'Arienzo C, Derbin G, Fagnoli J (2006) Discovery and preclinical studies of (R)-1-(4-(4-fluoro-2-methyl-1H-indol-5-yloxy)-5-methylpyrrolo[2, 1-f][1, 2, 4]triazin-6-yloxy)propan-2-ol (BMS-540215), an in vivo active potent VEGFR-2 inhibitor. *J Med Chem* 49:2143–2146
- Cai ZW, Zhang Y, Borzilleri RM, Qian L, Barbosa S, Wei D, Zheng X, Wu L, Fan J, Shi Z, Wautlet BS, Mortillo S, Jayaseelan R Sr, Kukral DW, Kamath A, Marathe P, D'Arienzo C, Derbin G, Barrish JC, Robl JA, Hunt JT, Lombardo LJ, Fagnoli J, Bhide RS (2008) Discovery of brivanib alaninate ((S)-((R)-1-(4-(4-fluoro-2-methyl-1H-indol-5-yloxy)-5-methylpyrrolo[2, 1-f][1, 2, 4]triazin-6-yloxy)propan-2-yl)2-aminopropanoate), a novel prodrug of dual vascular endothelial growth factor receptor-2 and fibroblast growth factor receptor-1 kinase inhibitor (BMS-540215). *J Med Chem* 51:1976–1980
- Carmeliet P, Jain RK (2000) Angiogenesis in cancer and other diseases. *Nature* 407:249–257
- Corbett T (1997) In vivo methods for screening and preclinical testing. Humana Press Inc, Totowa
- Davies B, Morris T (1993) Physiological parameters in laboratory animals and humans. *Pharm Res* 10:1093–1095
- de Mulder PH, Haanen JB, Sleijfer S, Kruit WH, Gietema JA, Richel DJ, Groenewegen G, Voest EE, van den Eertwegh AJ, Osanto S, Jansen RL, Mulders PF (2008) Angiogenesis inhibitors for the systemic treatment of metastatic renal cell carcinoma: sunitinib, sorafenib, bevacizumab and temsirolimus. *Ned Tijdschr Geneesk* 152:371–375
- Ellis LM, Fidler IJ (1996) Angiogenesis and metastasis. *Eur J Cancer* 32A:2451–2460
- Eric Masson AR, Kollia G, Syed S, Feltquate D, Mokliatchouk O, Velasquez L, Jonker D, Jayson G, Galbraith S (2008) Pharmacokinetics and pharmacodynamics of brivanib alaninate (BMS-582664), an oral dual inhibitor of VEGFR and FGFR signalling pathways in patients with advanced/metastatic solid tumors. 9th World Conference on Clinical Pharmacology and Therapeutics, Quebec, Canada
- Ferrara N (2002) VEGF and the quest for tumour angiogenesis factors. *Nat Rev Cancer* 2:795–803
- Folkman J, Klagsbrun M (1987) Angiogenic factors. *Science* 235:442–447
- Gibaldi M, Perrier D (1982) Pharmacokinetics. Marcel-Dekker, New York
- Grandinetti CA, Goldspiel BR (2007) Sorafenib and sunitinib: novel targeted therapies for renal cell cancer. *Pharmacotherapy* 27:1125–1144
- Gridelli C, Maione P, Del Gaizo F, Colantuoni G, Guerriero C, Ferrara C, Nicoletta D, Comunale D, De Vita A, Rossi A (2007) Sorafenib and sunitinib in the treatment of advanced non-small cell lung cancer. *Oncologist* 12:191–200
- Hiles JJ, Kolesar JM (2008) Role of sunitinib and sorafenib in the treatment of metastatic renal cell carcinoma. *Am J Health Syst Pharm* 65:123–131
- Lee FY, Borzilleri R, Fairchild CR, Kim SH, Long BH, Reventos-Suarez C, Vite GD, Rose WC, Kramer RA (2001) BMS-247550: a novel epothilone analog with a mode of action similar to paclitaxel but possessing superior antitumor efficacy. *Clin Cancer Res* 7:1429–1437
- Minagawa T, Kohno Y, Suwa T, Tsuji A (1995) Species differences in hydrolysis of isocarbacyclin methyl ester (TEI-9090) by blood esterases. *Biochem Pharmacol* 49:1361–1365
- Smith DA (2007) Do prodrugs deliver? *Curr Opin Drug Discov Devel* 10:550–559
- Stella VJ, Nti-Addae KW (2007) Prodrug strategies to overcome poor water solubility. *Adv Drug Deliv Rev* 59:677–694
- Wen Y, Remmel RP, Zimmerman CL (1999) First-pass disposition of (-)-6-aminocarbvir in rats. I. Prodrug activation may be limited by access to enzyme. *Drug Metab Dispos* 27:113–121